0888-8809/07/$15.00/0
Printed in U.S.A.

Molecular Endocrinology 21(10):2361–2377

doi: 10.1210/me.2007-0201

EXHIBIT J

The Nuclear Receptor-Coactivator Interaction Surface as a Target for Peptide Antagonists of the Peroxisome Proliferator-Activated Receptors

Niharika B. Mettu, Thomas B. Stanley, Mary A. Dwyer, Michelle S. Jansen, John E. Allen, Julie M. Hall, and Donald P. McDonnell

Department of Pharmacology and Cancer Biology (N.B.M., M.A.D., M.S.J., J.M.H., D.P.M.), Duke University Medical Center, Durham, North Carolina 27710; Department of Biochemical and Cellular Targets (T.B.S.), Molecular Discovery Research, GlaxoSmithKline, Research Triangle Park, North Carolina 27709; and Department of Chemistry (J.E.A.), Duke University, Durham, North Carolina 27708

The peroxisome proliferator-activated receptors (PPARα, PPARδ, and PPARγ) constitute a family of nuclear receptors that regulates metabolic processes involved in lipid and glucose homeostasis. Although generally considered to function as ligand-regulated receptors, all three PPARs exhibit a high level of constitutive activity that may result from their stimulation by intracellularly produced endogenous ligands. Consequently, complete inhibition of PPAR signaling requires the development of inverse agonists. However, the currently available small molecule antagonists for the PPARs function only as partial agonists, or their efficacy is not sufficient to inhibit the constitutive activity of these receptors. Due to the lack of efficacious antagonists that interact with the ligand-binding domain of the PPARs, we decided to target an interaction that is central to nuclear receptor-mediated gene transcription: the nuclear receptor-coactivator interaction. We utilized phage display technology to identify short LXXLL-containing peptides that bind to the PPARs. Analysis of these peptides revealed a consensus binding motif consisting of HPLLXXLL. Cross-screening of these peptides for binding to other nuclear receptors enabled the identification of a high-affinity PPAR-selective peptide that has the ability to repress PPARγ1-dependent transcription of transfected reporter genes. Most importantly, when introduced into HepG2 cells, the peptide inhibited the expression of endogenous PPARγ1 target genes, adipose differentiation-related protein and mitochondrial 3-hydroxy-3-methylglutaryl coenzyme A synthase 2. This work lends support for the rational development of peptidomimetics that block receptor-mediated transcription by targeting the nuclear receptor-coactivator interaction surface. (*Molecular Endocrinology* 21: 2361–2377, 2007)

THE PEROXISOME PROLIFERATOR-activated receptors α, δ, and γ (PPARα or NR1C1, PPARδ or NR1C2, and PPARγ or NR1C3) constitute a family of nuclear receptors that bind endogenous lipid ligands and regulate metabolic processes involved in lipid and glucose homeostasis (1, 2). PPARα is expressed at high levels in metabolically active tissues, reflecting its role in regulating genes that control fatty acid catabolism (3, 4). PPARδ is expressed ubiquitously and regulates a variety of processes, including wound healing, keratinocyte differentiation, and angiogenesis (5–8). Whereas PPARγ1 is expressed at low levels in many tissues and plays roles in proliferation and differentiation, PPARγ2 is highly adipose specific, where it functions as the master regulator of adipogenesis (9–11).

The PPARs heterodimerize with the retinoid X receptor (RXR) and activate transcription by binding to PPAR response elements (PPREs) that contain a direct repeat 1 (DR1) element in the promoters of target genes. Modulation of nuclear receptor transcriptional activity has traditionally been accomplished using agonists and antagonists that bind to the ligand-binding domain (LBD) of the receptor and induce conformational changes that either facilitate or inhibit transcription. The PPARs can bind a variety of fatty acid

First Published Online June 26, 2007

Abbreviations: aa, Amino acid; ADRP, adipose differentiation-related protein; AF-2, activation function-2; AR, androgen receptor; ASC-2, activating signal cointegrator 2; BAP, biotin acceptor peptide; 9cisRA, 9-cis retinoic acid; CMV, cytomegalovirus; DR1, direct repeat 1; ER, estrogen receptor; ERR, estrogen-related receptor; 5-FAM, 5-carboxyfluorescein; Gal4DBD, Gal4 DNA binding domain; HMGCS2, 3-hydroxy-3-methylglutaryl coenzyme A synthase 2; HRP, horseradish peroxidase; LBD, ligand-binding domain; LRH-1, liver receptor homolog-1; LXR, liver X receptor; NLA, normalized luciferase activity; PBST, PBS + 0.1% Tween 20; PEPCK, phosphoenolpyruvate carboxykinase; PGC, PPARγ coactivator; PPAR, peroxisome proliferator-activated receptor; PPRE, PPAR response element; PXR, pregnane X receptor; RAR, retinoic acid receptor; RXR, retinoic X receptor; Sf9 cells, *Spodoptera frugiperda* cells; SRC-1, steroid receptor coactivator 1; TR, thyroid receptor; TRAP, TR-associated protein.

***Molecular Endocrinology* is published monthly by The Endocrine Society (http://www.endo-society.org), the foremost professional society serving the endocrine community.**

EXHIBIT J

ligands, although it is not known which of these serve as true endogenous ligands (12–15). Synthetic agonists have also been developed for the PPARs: fibrates including clofibrate and urea-substituted thioisobutyric acids such as GW7647 are used to activate PPARα, carbaprostacyclin is an agonist of PPARδ, and thiazolidinediones including rosiglitazone and pioglitazone manifest their antidiabetic actions through activation of PPARγ1 and PPARγ2 (16, 17).

Because these receptors exhibit a high level of constitutive activity, inverse agonists are needed to repress both the ligand-activated and constitutive activities of these receptors. However, the available small molecule antagonists for the PPARs function only as partial agonists, or their efficacy is not sufficient to inhibit the constitutive activity. Thus, there is a well-defined need for small molecules that can be used to inhibit PPAR constitutive activity.

Due to difficulties in developing efficacious small molecule antagonists of the PPARs that target the LBD, we decided to approach the development of antagonists of these receptors by targeting the nuclear receptor-coactivator interaction. Binding of agonist to the PPARs facilitates a conformational change in the activation function-2 (AF-2) domain of the receptor, which promotes the displacement of corepressor proteins (18, 19). Agonist binding further enables the presentation of a hydrophobic coactivator binding pocket, which facilitates the interaction between the nuclear receptor and the canonical helical LXXLL motif found within many coactivators (20–22).

Using phage display technology, our laboratory has previously identified LXXLL-containing peptides that interact with the AF-2 of estrogen receptor α (ERα), estrogen receptor β (ERβ), androgen receptor (AR), vitamin D receptor, liver receptor homolog-1 (LRH-1), and estrogen-related receptor α (ERRα) (23–30). These respective peptides repress nuclear receptor-mediated transcription of transfected reporter genes. However, to our knowledge, peptide antagonists of nuclear receptors have not yet been successfully employed to block nuclear receptor-mediated regulation of endogenous target genes, an activity that must be demonstrated to validate the general approach.

Thus, the objectives of the current study were to 1) identify PPAR AF-2-interacting peptides using combinatorial phage display, 2) use these peptides to probe the nuclear receptor-coactivator interface, and 3) determine whether these peptides possess high enough affinity and selectivity to enable their use as peptide antagonists that repress AF-2-dependent reporter and endogenous gene transcription. The results of this study will assist in the development of peptidomimetics as PPAR modulators. Furthermore, they highlight the untapped potential of targeting the nuclear receptor-coactivator interface as a mechanism by which to modulate nuclear receptor transcriptional activity.

RESULTS

Selection of High-Affinity PPARγ1 Peptides Using Combinatorial Phage Display

To identify high-affinity peptides that interact with PPARγ1, we used combinatorial phage display technology to screen phage libraries expressing peptides as fusions with the M13 phage coat pili proteins (23, 25, 26). This method has been used previously by our laboratory to identify peptides that bind to ERα, ERβ, AR, vitamin D receptor, LRH-1, ERRα, and retinoic acid receptor α (RARα) (23–31). It has been established that PPARγ1 binds to LXXLL-containing coactivators, including p160 coactivators, PPARγ coactivator 1α (PGC-1α), and thyroid hormone receptor-associated protein complex 220 kDa component (TRAP220) (32–34). Therefore, we elected to identify PPARγ1-interacting peptides by screening a phage library expressing 19 amino acid peptides with a fixed LXXLL amino acid motif flanked by seven random amino acids on either side of the motif (X_7-LXXLL-X_7). Because RXRα ligands can activate PPARγ target genes, we hypothesized that the conformation of the AF-2 of PPARγ1 might be affected by its heterodimeric partner (35, 36). Therefore, to increase the diversity of the peptides identified, we screened for peptides that bound either to the PPARγ1/RXRα heterodimer on the PPRE from the adipocyte gene aP2, or to PPARγ1 that was immobilized directly on plastic.

To accomplish these objectives, highly purified recombinant PPARγ1 and RXRα were required. We produced full-length biotinylated human PPARγ1 (hPPARγ1) and RXRα (hRXRα) proteins by baculoviral overexpression in *Spodoptera frugiperda* (Sf9) cells and purified these biotinylated proteins on either monomeric avidin resin or streptavidin mutein matrix, as previously described for the purification of full-length androgen receptor (37). The purity of the recombinant hPPARγ1 and hRXRα proteins was evaluated by Coomassie blue staining (Fig. 1, A and B). The 475-amino acid hPPARγ1 protein fused to the 30-amino acid biotin acceptor peptide (BAP) was eluted from the column as a dominant 56-kDa band in the first eight fractions (Fig. 1A). A single band of the 462-amino acid hRXRα protein fused to BAP was detected at 55 kDa in four purified fractions (Fig. 1B).

To determine whether the proteins were functional with respect to their ability to heterodimerize on DNA, the hPPARγ1/hRXRα heterodimer was tested for its ability to bind to an aP2 PPRE oligonucleotide (Fig. 1C). The biotinylated oligonucleotide was immobilized on neutravidin-coated wells, and after excess neutravidin sites were blocked with biotin, hPPARγ1 and hRXRα were allowed to heterodimerize on the aP2 PPRE. GW7845, a nonthiazolidinedione agonist of PPARγ, and 9-cis retinoic acid (9cisRA), an agonist of RXRα, were used to induce active conformations in each receptor (38, 39). As expected, only the apo- and GW7845-bound hPPARγ1/hRXRα heterodimers

EXHIBIT J

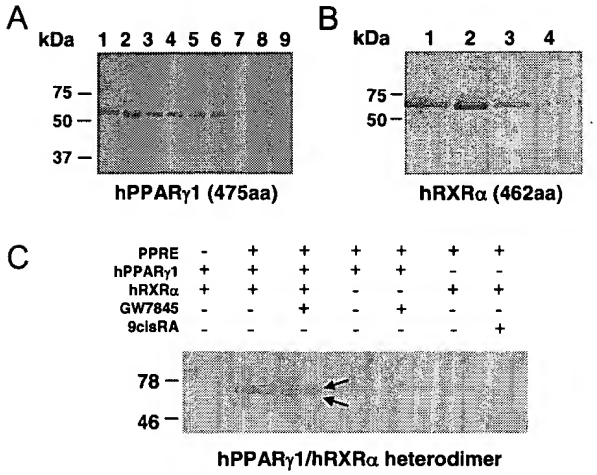

Fig. 1. Purification and Characterization of Purified hPPARγ1 and hRXRα

A and B, Full-length human hPPARγ1 and hRXRα proteins were overexpressed by infecting Sf9 insect cells with baculovirus expressing either hPPARγ1 or hRXRα. Proteins were purified by affinity chromatography using monomeric avidin resin and eluting with biotin-containing elution buffer. The elution fractions of hPPARγ1 (A, fractions 1–9) and of hRXRα (B, fractions 1–4) were loaded on reducing SDS-PAGE gels, and the purified proteins (fused to BAP) were visualized by Coomassie blue staining. C, The ability of hPPARγ1 and hRXRα to heterodimerize on an aP2 PPRE was tested *in vitro* in the absence or presence of PPARγ agonist GW7845 or RXRα agonist 9cisRA, as indicated. The bound proteins were boiled in sample loading buffer, loaded on a reducing SDS-PAGE gel, and visualized by Coomassie blue staining. *Arrows* indicate the two bands of the tight doublet formed by hPPARγ1 and hRXRα (each fused to BAP).

(lanes 2 and 3) were capable of binding to the aP2 PPRE, as evidenced by the tight double band seen on a Coomassie blue-stained gel (Fig. 1C). This result is in agreement with the known ability of the PPARγ1/RXRα heterodimer to bind to DNA in either the absence or presence of ligand (40). Binding of the heterodimer was DNA dependent (lane 1), and hPPARγ1 and hRXRα were incapable of binding to the aP2 PPRE as monomers (lanes 4–7).

These data confirm the production of full-length hPPARγ1 and hRXRα proteins, demonstrate their functionality, and validate our screening conditions. We used these proteins to perform three rounds of panning of an M13 phage library to identify LXXLL-containing peptides that interact with either hPPARγ1 in the presence of vehicle or rosiglitazone, or with the hPPARγ1/hRXRα heterodimer in the presence of vehicle, rosiglitazone, or rosiglitazone plus 9cisRA. The enrichment of PPARγ1-binding phage was demonstrated by a phage ELISA (data not shown).

Peptides Interact with the PPARs in Cells

To determine whether individual peptides from the phage pools could interact with PPARγ1 in a cellular environment, we used mammalian two-hybrid assays. DNA encoding peptides was PCR amplified from the pooled phage and shotgun ligated into a vector (pM5.1) that enabled the peptides to be expressed as fusion proteins at the N terminus of the Gal4 DNA binding domain (peptide-Gal4DBD). A total of 540 peptides were analyzed in mammalian two-hybrid assays performed in HepG2 cells for interaction with each of the PPARs fused to the VP16 transactivation domain. Mammalian two-hybrid analysis between five representative peptides (NBM131, NBM132, NBM225, NBM239, and NBM242) and VP16-PPARs showed robust interaction of each of these peptides with all of the PPAR subtypes (Fig. 2). The empty vector pM5.1 was used as a no-peptide control. No signal above background was detected when VP16 alone was used with any of these peptides, demonstrating that the interactions observed are PPAR dependent (data not shown).

Despite the fact that two of our five screens were performed in the absence of hRXRα protein, we found that 38% and 98% of all the peptides studied bound to VP16-RXRα in the presence of vehicle and 9cisRA, respectively (data not shown). This is not surprising because it is well known that LXXLL motifs bind to most nuclear receptors. To rule out the possibility, however, that these peptides may bind VP16-RXRα indirectly through binding to endogenous PPARs present in HepG2 cells, we repeated the analysis of several representative peptides with VP16-RXRα in HeLa cells, which do not express appreciable levels of the PPARs. The binding of the peptides to VP16-RXRα was reproduced in HeLa cells, suggesting that the binding to VP16-RXRα is, in fact, direct (data not shown).

Identification of an Extended PPAR Consensus Binding Motif

To determine the coactivator peptide-binding preferences of the PPARs, sequence analysis was performed on peptides that interacted with PPARγ1 in mammalian two-hybrid assays. Of the 130 peptides sequenced, 53 exhibited unique sequences (Fig. 3A). Alignment of these sequences revealed a strong consensus motif, HPLLXXLL (Fig. 3B). All of the sequences had a P in the −2 position with respect to the LXXLL motif, and only 13 had an amino acid other than H in the −3 position (M, N, S, or Y). More variability was observed for the −1 position with L being the most common amino acid, but other residues were observed as well (F, G, M, R, S, W, or Y) (Fig. 3, A and B). Interestingly, some flexibility was evident at the +4 and +5 positions, because peptides with AL, FL, ML, YL, and LI at these residues also interacted with PPARγ1 (Fig. 3, A and B).

To determine whether an unbiased, *i.e.* non-LXXLL-focused, screen would also select for peptides with the HPLLXXLL motif, we performed an additional screen of a peptide library with the format of SS-X_{16}-S

EXHIBIT J

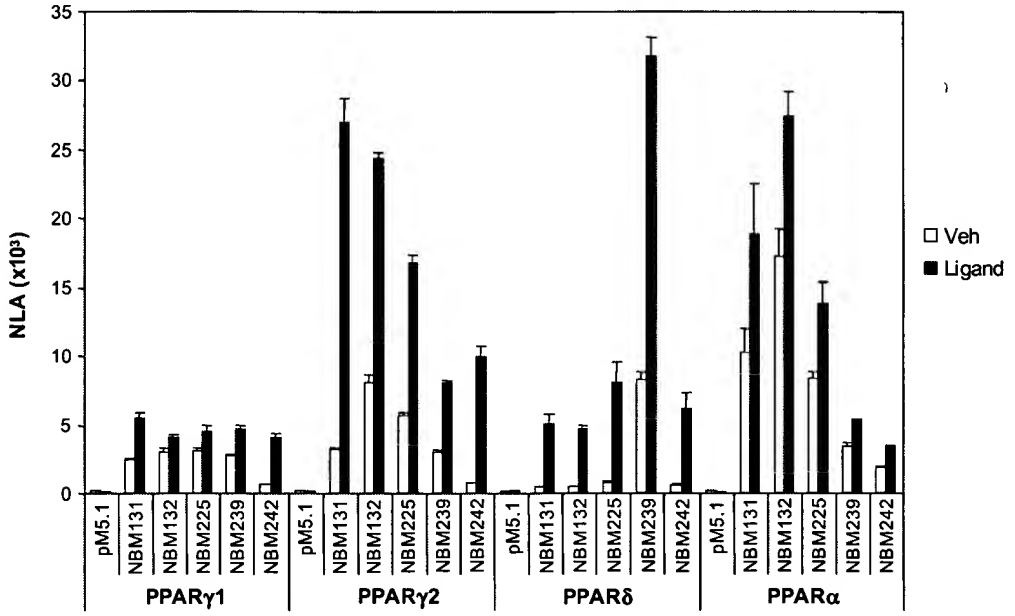

Fig. 2. Peptides Interact with the PPARs in Cells

Peptides (n = 540) were cloned as fusion proteins with the Gal4DBD. Mammalian two-hybrid analysis was performed to determine whether the peptide-Gal4DBD fusions could interact with the nuclear receptor fused to VP16 transactivation domain (VP16-NR) and activate transcription of a 5XGal4TataLuc3 reporter gene. Mammalian two-hybrid analysis of representative peptides was performed by transfecting HepG2 cells with VP16-GwA or VP16-GwA-NR (PPARγ1, PPARγ2, PPARδ, PPARα), 5XGal4TataLuc3, pM5.1 or pM5.1-peptide (NBM131, NBM132, NBM225, NBM239, NBM242), and CMV-βgal. *White bars* (□) were treated with vehicle (Veh), *black bars* (■) were treated with Ligand: 1 μM rosiglitazone (PPARγ1 and PPARγ2), 10 μM carbaprostacyclin (PPARδ), or 100 μM clofibrate (PPARα). Peptide sequences are as follows: ATTPPTQLHPLLTQFLRTD (NBM131), SSLEHPWLTMLLGKPHNMW (NBM132), PVFEHPRLVGLLVGTDIAS (NBM225), ILEEHPLLASLLTETSRGM (NBM239), SLEAHPLLSALLQDQMGGD (NBM242). Results are expressed as NLA (normalized with βgal for transfection efficiency) ± SEM per triplicate sample of cells.

(16 random residues flanked by SS at the N terminus and S at the C terminus). In addition, we also analyzed short peptides encoded by out-of-frame cDNAs recovered from another screen using several T7 cDNA libraries (Jansen, M. S., and D. P. McDonnell, unpublished data). Interestingly, both of these essentially random peptide screens also yielded peptides that contain sequences resembling the eight amino acid consensus (Fig. 3A).

The peptide libraries used in the screen consist of 19 amino acids; however, the consensus was defined by only eight amino acids (Fig. 3B). To test whether the eight-amino acid consensus motif is sufficient for binding to PPARγ1, the sequence corresponding to the motif derived from NBM242 was cloned as a fusion protein with the Gal4DBD. Mammalian two-hybrid analysis revealed that the eight-amino acid motif, HPLLSALL, is sufficient for binding to PPARγ1 in a ligand-inducible manner (Fig. 3C).

We performed alanine scanning mutagenesis using the peptide NBM242 as a template to determine the contribution of each conserved residue in the consensus motif to PPARγ1 binding (Fig. 4A). Setting the first leucine of the LXXLL motif as position 1, the mutation number indicates the amino acid position at which the *in situ* amino acid was mutated to alanine (Fig. 4A). All mutants were expressed as demonstrated by Western blot analysis with an anti-Gal4DBD antibody (Fig. 4B).

As expected, all three leucines within the LXXLL motif were indispensable for binding to the PPARs (Fig. 4C). Two control mutations upstream of the motif, mutation −5 and −6, retained binding to the PPARs. Mutational analysis revealed the importance of the −3 histidine, the −2 proline, and the −1 leucine for the binding of NBM242 to PPARγ1, PPARα, and PPARδ. Interestingly, mutation −6 increased the ligand-independent interaction of NBM242 with PPARγ1 and PPARα to almost the level of interaction seen in the presence of their ligands.

The importance of these residues for binding to other nuclear receptors is more variable: mutation −3 permitted NBM242 to retain binding to RXRα, ERα, and ERRα, mutation −2 caused reduced binding, and mutation −1 caused reduced binding to RXRα and ERα but enabled NBM242 to retain some binding to ERRα (Fig. 4C). Unexpectedly, we found that the −6 leucine appears to be important for binding to ERα, because mutation of this amino acid drastically reduced binding of NBM242 to ERα. Collectively, these results demonstrate that although the −3 histidine, −2 proline, and −1 leucine are all important for NBM242 to bind to the PPARs, the −3 histidine is not required

EXHIBIT J

A

X_7-LXXLL-X_7 Library (Focused)
ISYE HPLLTGLL LEQRHVD
LDGDVSKL HPLLVNFL KGD
VESS HPLLVGLL GKQQATV
SEGL HPLLTALL APQVTQW
ALHDQQSL HPLLAEAL LRD
PMVQ HPWLVGLL VSAEGVS
DLAEPVKL HPLLSMYL SNL
VAQM HPGLSELL LASHFHQ
VHVT MPFLTSLL TGQPTSV
MPLH SPYLLSLL TGSGQSL
VDLE YPMLVHLL QYGRELS
PVET HPRLLKLL TRAEYPM
TEVT HPLLASLL QYGVQVS
ATTPPTQL HPLLTQFL RTD
SSLE HPWLTMLL GKPHNMW
PVTA YPMLAELL LPTGQLR
MSQSVSDL HPLLGLLL TAD
VATN HPWLTMLL NGQASGE
PLAL HPLLASLL DPGRQLV
TQME YPLLTQLL GGRTMEE
LLEA HPLLTGLL GASSLEL
ILEE HPLLASLL TETSRGM
LSQE YPWLTRLL DSGQLGS
TWLE YPLLTDLL LPSWRQD
SAAD HPSLLRLL TGDFPYE
ISYE HPLLTGLL LDSVMW
LELEATSL HPLLLQLI KQV
PVFE HPRLVGLL VGTDIAS
LGES HPLLMQLL TENVGTH
VEE NPLLLEML LSASKASS
MVAQ NPLLGGLL LGSMDTM
PTS SPLLLDLL LGRPVETV
PFYT HPMLSSLL LGPPSMT
PTVE HPMLSSLL RGAANEF
TVVQ HPWLTGLL IGSGQDA
SLEA HPLLSALL QDQMGGD
PLSD HPMLLELL NHNSMRN
HQE HPLLLHML LGGSQEVE
NHET HPLLSKLL LSPLEQT
MSD HPLLLSYL LETTAVLP
GVLD HPLLFQLL SSETRVL
IAGE HPMLWGLL RAGGLPE
PADN MPLLRTLL LGSGIEV
TIDS HPMLHSLL SQRGLVA
VAHT HPLLVGLL KGSITGP
ALSD SPLLLSLL LGHPDWQ
TYVD HPLLAELL LGEVGMN
ADGSPMEL HPLLSRLI TAP
PVEG HPWLLGLL VGAEVDV
ALSSPSDL NPLLTSLL SQS
MTLE HPGLTALL ASQSLMG
SVDQ HPMLMDLL TGLKRAE
MVE HPRLLSLL LDRSDVPM

T7 cDNA Libraries (Random)
SPLHPLLLALLLGRGAQP
X_{62}-KELTHPLLVSLLLKEKQDG
X_{10}-KELTHPLLVSLLLKEKQDG
X_1-VWSLHGLLAQLLSQPPSAS-X_{19}
X_1-EGAGHGLLLALLRGSGLPG-X_{14}
X_{24}-SLSRHGLLFALLSGQQKKK-X_{23}
X_{21}-FTSMSPLLRCLLSISYPGSSPLLRTLLQESCTLS-X_{21}
X_{21}-FTSMSPLLRCLLSISYPGS
X_{16}-GRRHLPLLRLLLARQGGGG-X_1
X_1-PACRNPILTNLLKTQKFY
X_9-KAITNPILTHLLLSVKSSS-X_{25}
X_1-PACRNPILTNLLKTPEILL-X_3
X_6-QAQQKSLLQQLLTE
X_9-PLSPGSLLYQLLTLGPLNPSLPGSHLLSLLLS
SLLSALLRGAQGQV-X_7

SS-X_{16}-S Library (Random)
SSSLLHPLLVDLLQMGGASS
SSSSVLNPLLAELLASGSSS
SSSYLLDLLLGTSDVTTNVS

B

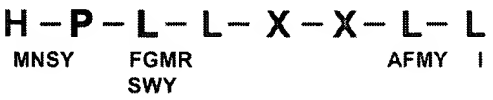

C

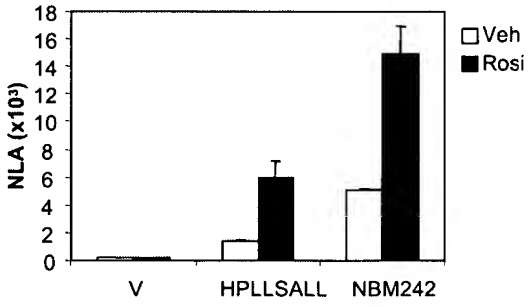

Fig. 3. Identification of an Extended PPAR Consensus Binding Motif

A, Sequence analysis of PPARγ1-interacting peptides isolated from two M13 peptide screens using X_7-LXXLL-X_7 and SS-X_{16}-S libraries, and from screens of T7 cDNA libraries. X_n denotes n number of amino acids. Peptides from the X_7-LXXLL-X_7 library have the fixed LXXLL motif shown in *red*, unless it is *underlined* in *black*. The extended part of the PPAR consensus binding motif is shown in *blue*. B, The sequences revealed an extended consensus binding motif consisting of eight amino acids. The other amino acids found occasionally in place of the −3 H, −1 L, +4 L, and +5 L are indicated *below* the motif. C, The eight-amino acid consensus motif from NBM242 was cloned as a fusion to the Gal4DBD, and the ligand-inducible interactions of vector (V), this eight-amino acid motif, HPLLSALL, as well as NBM242 with VP16-PPARγ1 were evaluated by mammalian two-hybrid analysis. HepG2 cells were transfected with VP16-PPARγ1, 5XGal4TataLuc3, pM5.1 (V) or pM5.1-peptide (HPLLSALL and NBM242), and CMV-βgal. *White bars* (□) were treated with vehicle (Veh), *black bars* (■) were treated with 1 μM rosiglitazone (Rosi). Results are expressed as NLA (normalized with βgal for transfection efficiency) ± SEM per triplicate sample of cells.

EXHIBIT J

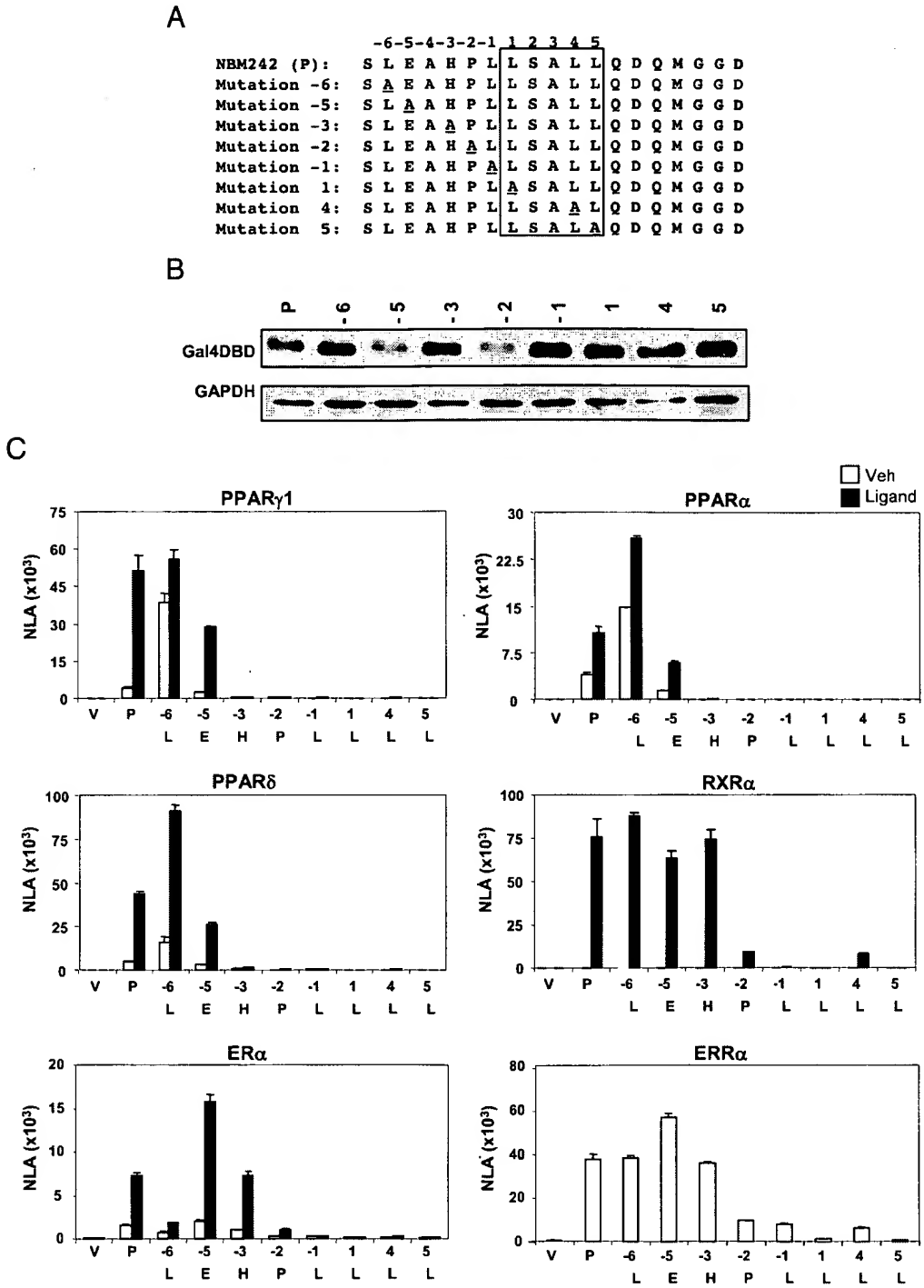

Fig. 4. The −3 Histidine Is Important for Binding to PPARs But Not to Other Nuclear Receptors

A, Alanine scanning was performed by site-directed mutagenesis of individual amino acids within the peptide NBM242 (P). The position of the amino acid mutations is indicated *above* the NBM242 sequence, using the first L of the LXXLL motif as position 1. The alanine mutation is *underlined* in each sequence, and the LXXLL motif is *boxed*. B, Expression of the mutants was confirmed by Western blot analysis using an anti-Gal4DBD primary antibody and an antirabbit IgG HRP-conjugated secondary antibody. GAPDH was used as a loading control. C, The mutants generated as depicted in panel A were evaluated by mammalian two-hybrid analysis for binding to VP16-PPARγ1, VP16-PPARα, VP16-PPARδ, VP16-RXRα, VP16-ERα, and VP16-ERRα. HepG2 cells were transfected with VP16-nuclear receptor, 5XGal4TataLuc3, pM5.1-peptide, and CMV-βgal. The mutation is indicated on the x-axis, where V is vector, P is the NBM242 peptide, and the number corresponds to the mutation number. The identity of the amino acid that was mutated is indicated *beneath* the mutation number. *White bars* (□) were treated with vehicle (Veh), *black bars* (■) were treated with ligand (1 μM rosiglitazone for PPARγ1, 100 μM clofibrate for PPARα, 10 μM carbaprostacyclin for PPARδ, 1 μM 9cisRA for RXRα, or 100 nM 17β-estradiol for ERα). Results are expressed as NLA (normalized with βgal for transfection efficiency) ± SEM per triplicate sample of cells. GAPDH, Glyceraldehyde-3-phosphate dehydrogenase.

EXHIBIT J

for the interaction of this peptide with other nuclear receptors including RXRα, ERα, and ERRα.

Stabilization of Peptides Occurs through Interaction of the −3 Histidine with K319 and E471 of PPARγ1

The importance of the −3 histidine was interesting, because this position has not been shown in previous studies to be important for interacting with other nuclear receptors (23–30). To understand how PPARγ1 may be interacting with this unique residue of the motif, we modeled the consensus peptide from NBM242 (HPLLSALL) with the PPARγ LBD using the previously published structure of the PPARγ/RXRα heterodimer complexed to 9cisRA, rosiglitazone, and a peptide derived from the p160 coactivator steroid receptor coactivator 1 (SRC-1), containing a single LXXLL motif (41, 42). Based upon the modeling, the histidine within the motif is predicted to form a salt bridge with K319 within helix 4 and one of the charge clamp residues, E471, within helix 12 of PPARγ1 (Fig. 5A).

To determine the importance of K319 and E471 for stabilizing the interaction with PPAR-interacting peptides, each of these residues within PPARγ1 was mutated to alanine (K319A and E471A). Expression of the mutants was confirmed by Western blot analysis using an anti-PPARγ antibody (Fig. 5B). Mammalian two-hybrid analysis was performed to test the ability of the mutated PPARγ1 receptors to bind to NBM242 (Fig. 5C, *left*). As expected, PPARγ with the charge clamp glutamate mutation, E471A, completely lost the ability to interact with NBM242. K319A also destabilized but

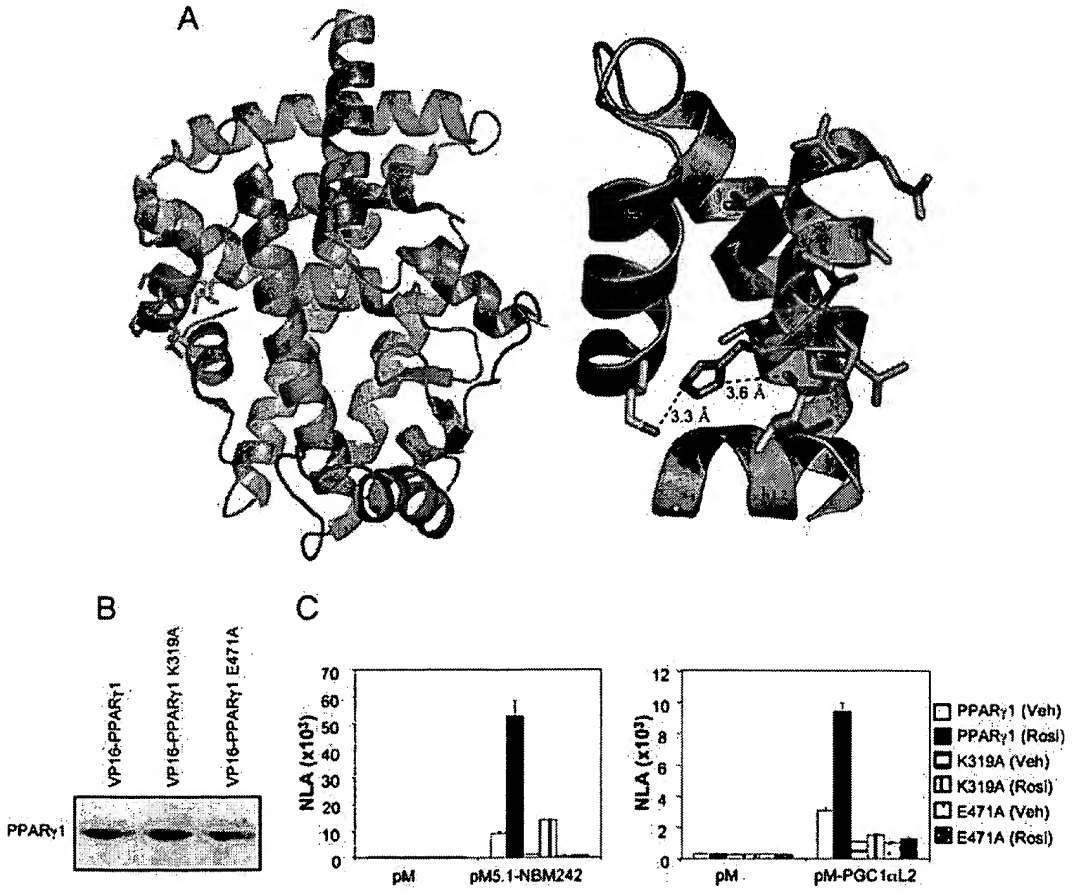

Fig. 5. Molecular Modeling of the NBM242 Peptide with PPARγ LBD

A, The motif from the NBM242 peptide (HPLLSALL) was modeled using the published structure [PDB Code: 1FM6, Gampe *et al.* (42)] of the PPARγ/RXRα heterodimer complexed to 9cisRA, rosiglitazone, and a peptide derived from the coactivator SRC-1, containing a single LXXLL motif (*left*) (41). Examined more closely (*right*), the histidine of the motif is predicted to form salt bridges with K319 in helix 4 and E471 in helix 12 of PPARγ1. B, VP16-PPARγ1 K319A and E471A mutants were made, and expression was confirmed by Western blot analysis with an anti-PPARγ primary antibody and an antimouse IgG HRP-conjugated secondary IgG antibody. C, Interaction of the wild-type PPARγ1 (PPARγ1), PPARγ1K319A (K319A), and PPARγ1E471A (E471A) with NBM242 (*left*) and PGC-1α L2 peptide (PGC1αL2, EAEEPSLLKKLLLAPANTQ, *right*) was tested by mammalian two-hybrid analysis in the presence of vehicle (Veh) or 1 μM rosiglitazone (Rosi). HepG2 cells were transfected with VP16 or VP16-PPARγ1 (PPARγ1, K319A, or E471A), 5XGal4TataLuc3, peptide (pM, pM-PGC1αL2, or pM5.1-NBM242), and CMV-βgal. Results are expressed as NLA (normalized with βgal for transfection efficiency) ± SEM per triplicate sample of cells.

EXHIBIT J

did not abolish the binding of NBM242 to PPARγ1, suggesting that there may also be other residues that are important for further stabilizing the interaction of PPARγ1 with the peptide.

Mammalian two-hybrid analysis with the 19-amino acid peptide centered around the second LXXLL motif of PGC-1α (PGC1αL2) also demonstrated that both the K319A and E471A mutations of PPARγ1 abrogated the interaction of the PGC1αL2 peptide with PPARγ1. These data suggested that the peptides we identified bind to PPARγ1 in a manner similar to known PPARγ1 coactivators such as PGC-1α (Fig. 5C, *right*).

PPAR Peptides Compete with Coactivators to Inhibit PPRE-Containing Reporter Gene Expression

The suggestion that our peptides might bind to PPARγ1 in a manner similar to known coactivators suggested that they may be able to compete with coactivators for binding to PPARγ1. We tested, in a competition ELISA, whether a synthetic peptide, NBM239, could compete away the binding of the coactivator, activating signal cointegrator 2 (ASC-2), from PPARγ1. This was achieved by adding to wells containing immobilized hPPARγ1 increasing amounts of NBM239 with a fixed pfu of a T7 phage expressing the nuclear receptor AF2-interacting fragment of ASC-2 (amino acids 254–321). After incubation and washing, the amount of ASC-2 retained was detected using anti-T7 phage horseradish peroxidase (HRP)-conjugated antibody. NBM239 was able to compete away the coactivator-phage from hPPARγ1 in a dose-dependent manner, demonstrating that, *in vitro*, these peptides are avid competitors of coactivator binding (Fig. 6A).

Given this finding, we hypothesized that these peptides might be capable of functioning as peptide antagonists of PPARγ1 transcriptional activity by blocking receptor-coactivator binding in cells. Thus, transcriptional interference assays were performed by testing the ability of PPAR-interacting peptides to repress PPARγ1-mediated transcription of transfected DR1-luciferase (DR1-Luc) or phosphoenolpyruvate carboxykinase (−2000/+73)-luciferase (PEPCK-Luc) reporters. As a comparison, we also tested the 19-amino acid peptide PGC1αL2, which contains the PPARγ1-interacting domain of the coactivator PGC-1α, in transcriptional interference assays.

Transfection of PGC1αL2, NBM239, and NBM242 all repressed PPARγ1 transcription of both DR1-Luc and PEPCK-Luc in a dose-dependent manner (Fig. 6B). The relative competitive potencies of these three peptides could be attributed to differences in affinity for PPARγ1 or protein expression levels. In addition to inhibiting rosiglitazone-activated transcription, NBM239 is capable of inhibiting the high constitutive activity of PPARγ1 by 50% on DR1-Luc (Fig. 6B, panel 3) or by 75% on PEPCK-Luc (Fig. 6B, panel 4). The specificity of inhibition was demonstrated by the fact that basal expression of the reporter genes in the absence of cotransfected PPARγ1 was not affected by the peptides (data not shown). In contrast, a previously identified peptide that does not bind to PPARγ1, H60, has no effect on PPARγ1 transcription on either DR1-Luc or PEPCK-Luc (data not shown). Thus, these peptides represent novel antagonists of PPARγ1 that function by blocking coactivator recruitment to the receptor and inhibiting transcription of transfected reporters.

PPAR Peptides Have Higher Affinities for PPAR LBDs Than Coactivator Peptides

To determine whether these peptides exhibit the high affinity for the PPARs that would facilitate their use as peptide antagonists of endogenous genes, we performed fluorescence polarization assays to establish the affinity of selected peptides for the PPARs. We first assessed the affinity of LXXLL motifs from PGC-1α and TRAP220 for the PPAR LBDs. The 5-carboxyfluorescein (5-FAM)-labeled peptides containing nuclear receptor interaction motifs from PGC-1α and TRAP220 bind the PPAR LBDs with distribution constant (K_D) values ranging from 732 to 2754 nM, similar to K_D determined for the ERα LBD (Fig. 7A, *right graph* and *table*).

We then determined the affinities of the following 5-FAM-labeled peptides for PPARα, PPARγ, PPARδ, and ERα LBDs in the absence of ligand: NBM131, NBM239, and NBM131mut (a control peptide consisting of the NBM131 peptide with the LXXLL mutated to AXXAA). NBM131mut had no detectable affinity for any LBD tested (data not shown). NBM131 had K_D values of 87, 77, and 308 nM, and NBM239 had K_D values of 78, 78, and 48 nM for PPARα, PPARγ, and PPARδ LBDs, respectively (Fig. 7A, *left* and *middle graphs*, and *table*). In contrast, the K_D values of NBM131 and NBM239 for ERα LBD were >20,000 and 8319 nM, respectively. The affinity measurements did not appreciably differ in the presence of ligands for each of the receptors (data not shown). These affinity measurements revealed that the peptides we identified have 1 order of magnitude higher affinity and selectivity for the PPARs than coactivator peptides, highlighting their potential utility as peptide antagonists of endogenous PPAR target genes.

PPAR-Selective Peptide Antagonist, NBM131, Represses Endogenous Gene Transcription in HepG2 Cells

The ability of the PPAR peptide antagonists to efficiently repress transcription on DR1-Luc and PEPCK-Luc reporter genes (Fig. 6B) and their high affinity (Fig. 7A) suggested that they might be able to function as antagonists of endogenous target genes. We screened the 540 peptides we had cloned to identify those that display a low level of binding to other receptors in mammalian two-hybrid assays. In this man-

EXHIBIT J

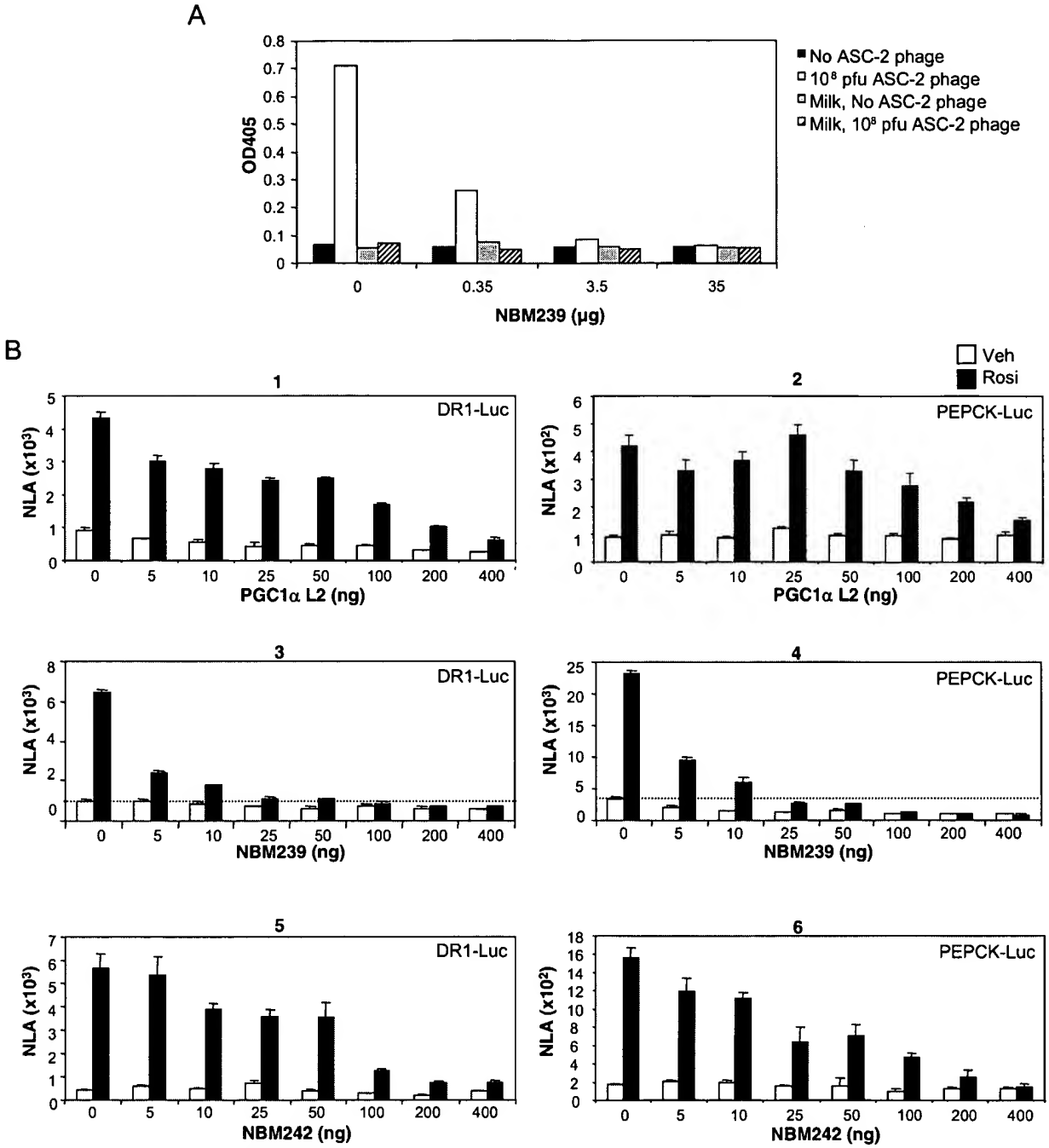

Fig. 6. PPAR Peptides Compete with Coactivators to Inhibit PPRE-Containing Reporter Gene Expression

A, Competition ELISA using synthetic NBM239 to compete away a coactivator-phage expressing the nuclear receptor-interacting domain of ASC-2 (amino acids 254–321, ASC-2 phage) from purified PPARγ1 *in vitro*. B, Effect of PGC1αL2 (panels 1 and 2), NBM239 (panels 3 and 4), and NBM242 (panels 5 and 6) on PPARγ1 transcription of transfected DR1-luciferase (DR1-Luc, *left panels*) and PEPCK-luciferase (PEPCK-Luc, *right panels*) reporter genes in cis-trans assays. HeLa cells were transfected with pcDNA3.1nV5-PPARγ1, DR1-Luc or PEPCK-Luc, increasing amounts of the pM-peptide or pM5.1-peptide indicated on the x-axis, and CMV-βgal. Peptide amounts were balanced with empty pM or pM5.1 vector. *White bars* (□) were treated with vehicle (Veh); *black bars* (■) were treated with 1 μM rosiglitazone (Rosi). Results are expressed as NLA (normalized with βgal for transfection efficiency) ± SEM per triplicate sample of cells.

ner, we identified a PPAR-selective peptide, NBM131, which interacts with the PPARs (Fig. 2), but does not interact with most other nuclear receptors in the absence of exogenous ligands (supplemental Fig. 1A published as supplemental data on The Endocrine Society's Journals Online web site at http://mend.endojournals.org). As expected, transfected NBM131 efficiently inhibited PPARγ1 transcriptional activity on

EXHIBIT J

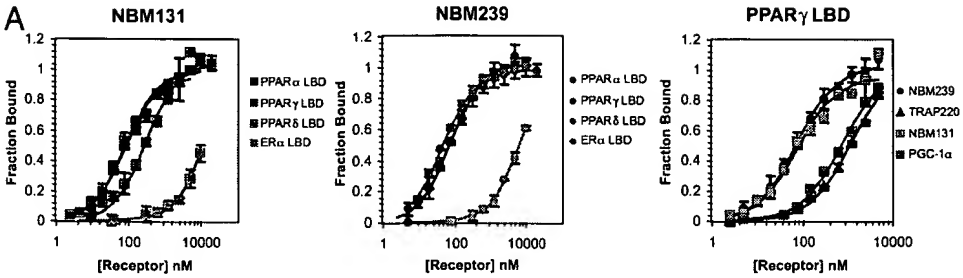

Protein	NBM131 K_D (nM)	NBM239 K_D (nM)	PGC-1α K_D (nM)	TRAP220 K_D (nM)
PPARα LBD	87	78	1477	2754
PPARγ LBD	77	78	732	1156
PPARδ LBD	308	48	836	1325
ERα LBD	>20000	8319	1727	2683

B

Peptide	Amino acid sequence
NBM131	ATTPPTQLHPLLTQFLRTD*
NBM131mut	ATTPPTQAHPAATQFLRTD*
NBM239	ILEEHPLLASLLTETSRGM*
PGC-1α	EAEEPSLLKKLLLAPANTQ*
TRAP-220	GHGEDFSKVSQNPILTSLLQITGNG

Fig. 7. PPAR Peptides Have Higher Affinities for PPAR LBDs Than Coactivator Peptides

A, Affinities (K_D) of 5-FAM-labeled NBM131 (*left graph*) and NBM239 (*middle graph*) for the LBDs of PPARα, PPARγ, PPARδ, and ERα were determined by fluorescence polarization in the absence of ligand. Affinities of the nuclear receptor interaction domains of PGC-1α and TRAP220 were also determined for each of the LBDs, and the data are presented graphically for PPARγ LBD (*right graph*). The K_D for each peptide is indicated in the *table below* the *graphs*. Data presented are the average of two independent experiments. B, Amino acid sequences of PPAR-interacting peptides used in this experiment. *, The fluorescent peptides synthesized for use in fluorescence polarization assays had an extra cysteine at the C terminus.

both DR1-Luc and PEPCK-Luc reporter genes (Fig. 8A, *top*), but had no effect on the transcriptional activity of other nuclear receptors (supplemental Fig. 1, B and C).

We created a control version of this peptide, NBM131mut4, which has the LXXLL mutated to LXXAA. Mutations of the leucines within the LXXLL motif disrupted the ability of NBM131mut4 to interact with any of the PPARs (supplemental Fig. 1D). Accordingly, NBM131mut4 lacked the ability to repress PPARγ1 transcription of DR1-Luc and PEPCK-Luc (Fig. 8A, *bottom*).

We generated adenoviruses expressing NBM131 and NBM131mut4 fused to the Gal4DBD and showed that both peptides were expressed at comparable levels when HepG2 cells were infected with the adenoviruses, as illustrated by Western blot analysis of the whole cell extracts using an anti-Gal4DBD antibody (Fig. 8B). We further confirmed that the adenoviral-mediated expression of NBM131, but not NBM131mut4, potently represses transcription of a transfected DR1-Luc reporter gene, in a manner similar to the transfected peptide (supplemental Fig. 1E).

To address whether NBM131 could function as a peptide antagonist of endogenous PPAR-regulated gene expression, we used quantitative PCR to confirm the expression of several known PPAR targets in our model system, HepG2 cells. Adipose differentiation-related protein (ADRP) has been shown to be regulated by agonists of all three PPAR subtypes *in vitro* and *in vivo*, and, as expected, we found that rosiglitazone induces the expression of ADRP (data not shown) (43). 3-Hydroxy-3-methylglutaryl coenzyme A synthase 2 (HMGCS2) is a well-characterized PPARα target gene in the liver that produces the mitochondrial HMGCS2 enzyme, which catalyzes a key reaction in the ketogenesis pathway (44). As expected, we found that GW7647, a PPARα agonist, induces the expression of HMGCS2 (data not shown). However, interestingly, we found that HMGCS2 can be induced to an even higher degree by rosiglitazone (data not shown).

To determine whether our PPAR-selective peptide, NBM131, could inhibit the expression of these PPARγ1 target genes, we infected HepG2 cells with the adenoviruses expressing either NBM131 or NBM131mut4. We found that introduction of NBM131 resulted in inhibition of the rosiglitazone-stimulated induction of both ADRP and HMGCS2, as compared with cells infected with the control adenovirus NBM131mut4 (Fig. 8C). In conclusion, we have been able to use a high-affinity 19-amino acid LXXLL-containing peptide to inhibit transcription of endogenous PPARγ1 target genes, further validating the approach of targeting the nuclear receptor-coactivator interaction as a means by which to modulate nuclear receptor transcriptional activity.

EXHIBIT J

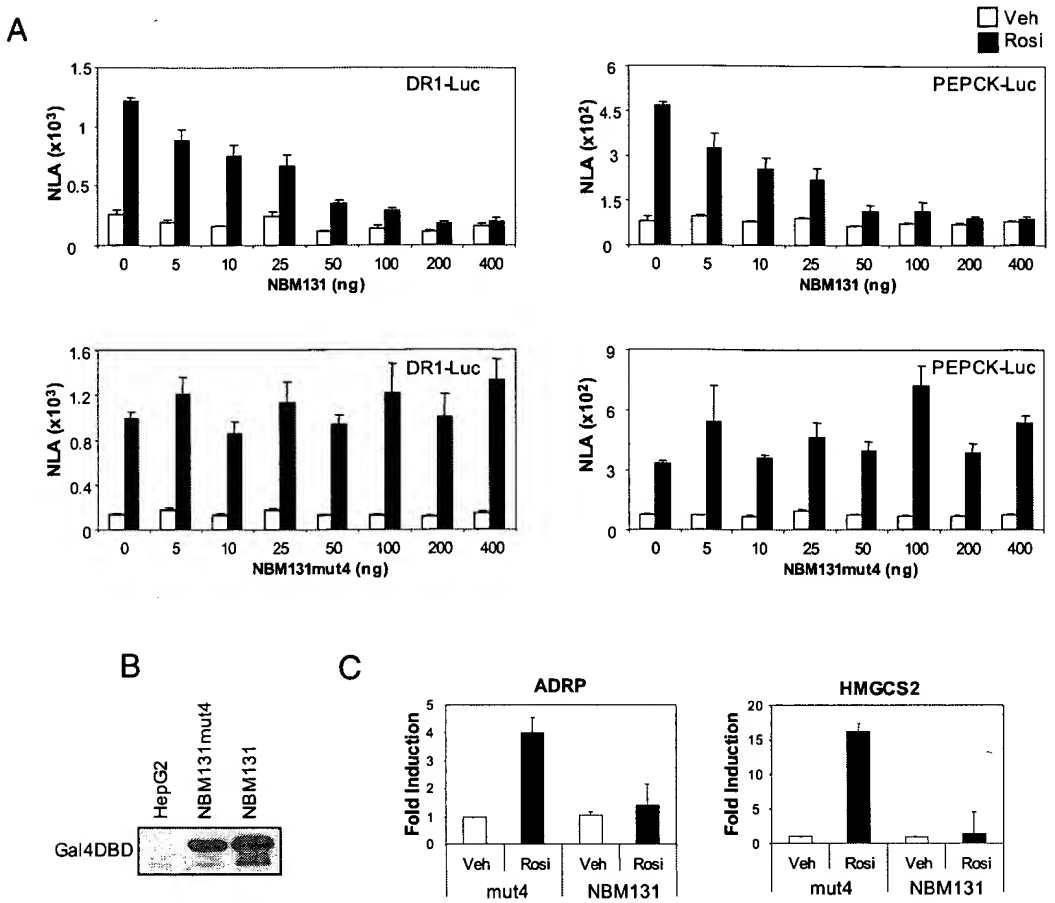

Fig. 8. PPAR-Selective Peptide Antagonist, NBM131, Represses Endogenous Gene Transcription in HepG2 Cells

A, Effect of NBM131 (*top panels*) and NBM131mut4 (*bottom panels*) on PPARγ1 transcription of transfected DR1-luciferase (DR1-Luc, *left panels*) and PEPCK-luciferase (PEPCK-Luc, *right panels*) reporter genes in cis-trans assays. HeLa cells were transfected with pcDNA3.1nV5-PPARγ1, DR1-Luc or PEPCK-Luc, increasing amounts of the pM5.1-peptide indicated on the x-axis, and CMV-βgal. Peptide amounts were balanced with empty pM5.1 vector. *White bars* (□) were treated with vehicle (Veh); *black bars* (■) were treated with 1 μM rosiglitazone (Rosi). Results are expressed as NLA (normalized with βgal for transfection efficiency) ± SEM per triplicate sample of cells. B, Expression of peptides in HepG2 cells infected with adenoviruses expressing NBM131 or NBM131mut4 by Western blot analysis using an anti-Gal4DBD primary antibody and an antirabbit IgG HRP-conjugated secondary antibody. C, Effect of NBM131 and NBM131mut4 on endogenous target gene expression of adipocyte differentiation-related protein (ADRP) and 3-hydroxy-3-methylglutaryl coenzyme A synthase 2 (HMGCS2) by real-time RT-PCR. *White bars* (□) were treated with vehicle (Veh); *black bars* (■) were treated with 1 μM rosiglitazone (Rosi). Sequences of primers of genes used are indicated in supplemental Fig. 1F. Results are normalized to the NBM131mut4-infected, vehicle-treated sample.

DISCUSSION

Nuclear receptor-mediated target gene expression is a multistep process that involves ligand binding, association with target gene promoters, coactivator recruitment, and assembly of the transcriptional machinery. Although each step in this process can be targeted for the development of new drugs, most of the current drugs target only the initial step. In the past, we have tried to target coactivator recruitment, and to this end, we have identified selective peptides for a number of nuclear receptors and used them to inhibit nuclear receptor-mediated activation of transfected reporter genes in cells. However, we have not been able to use this approach to inhibit endogenous target gene expression. This difficulty is primarily thought to be due to the low affinity of peptides for their respective receptors. In the current study, we have successfully identified peptides with nanomolar affinity for the PPARs, and most importantly, we have used these peptides to inhibit transcription of endogenous PPAR target genes. Notably, one of our peptide antagonists, NBM131, inhibited the rosiglitazone-induced transcription of ADRP and HMGCS2.

Although our studies were focused on PPAR, it is clear that the general approach of blocking nuclear receptor-coactivator interactions can be applied to target other receptors and biologies. Aromatic β-aminoketones have been identified that covalently bind to thyroid receptor (TR) in a pocket distinct from the

EXHIBIT J

agonist-binding pocket, and these compounds inhibit TR-coregulator interaction *in vitro* and TR transcriptional activity on a transfected reporter (45). Additionally, ketoconazole, a commonly used antifungal drug, inhibits the interaction between pregnane X receptor (PXR) and SRC-1 *in vitro* and *in vivo*, leading to an inhibition of PXR-mediated drug metabolism *in vivo* (46). These compounds each bind to the receptor at sites distinct from the agonist-binding pocket and inhibit the interaction between nuclear receptors and coactivators, thereby blocking receptor-mediated transcription. These studies support our hypothesis that the nuclear receptor-coactivator interaction can be targeted to modulate receptor-mediated transcription. Furthermore, they demonstrate the applicability of this approach to nuclear receptors other than the PPARs.

This approach may be of clinical value in the setting of hormone-dependent cancers. For example, the mainstay of therapy in breast and prostate cancers is anti-hormone therapy; however, the progression of initially anti-hormone-responsive cancers to an anti-hormone-refractory state is common, necessitating the development of drugs that can block the transcriptional activity of nuclear receptors via mechanisms other than classic antagonism. The onset of resistance to anti-hormone therapy highlights the unmet need for mechanistically distinct antagonists. The significance of the nuclear receptor-coactivator interaction for nuclear receptor-mediated activation of gene transcription suggests that targeting this interface offers a novel and complementary mechanism by which to inhibit a receptor's transcriptional activity. This approach may be used for the treatment of refractory tumors or disease processes in which a competitive antagonist of the receptor is difficult to develop.

The results of this study should serve as a prototype for the rational development of peptidomimetics as a mechanism by which to modulate nuclear receptor activity. Small molecule peptidomimetics obviate some of the disadvantages of using peptides as drugs, *e.g.* low bioavailability, poor transport into the bloodstream, and rapid excretion (47). By defining the local and global conformational parameters of a biologically active peptide and optimizing the constituents of the backbone amino acids, a peptidomimetic can be developed that retains the peptide's effect with improved stability, bioavailability, and transport across cell membranes (47, 48). Techniques such as polyarginine modification or the addition of other cell-penetrating peptides can facilitate transport (49, 50). However, each of these approaches limits oral bioavailability and increases the costs of pharmaceutical production. Limiting the peptide length is also an important consideration in designing peptidomimetics with increased stability and transport. We have demonstrated that we are able to narrow down a 19-amino acid peptide to eight amino acids and still retain binding to PPARγ1 in the absence and presence of ligand. Although this eight-amino acid peptide was not capable of inhibiting PPARγ1 transcription (data not shown), we believe that with further optimization, it may be possible to develop peptidomimetics targeting this interaction.

It has been previously demonstrated that the dipeptide G3335 (H-Trp-Glu-OH) is a PPARγ antagonist that blocks the ability of rosiglitazone to stimulate an interaction between the PPARγ and RXRα LBDs (51). However, the specificity, mechanism, and effect on endogenous target genes of G3335 have not been characterized. In assays measuring the PPARγ LBD-CREB binding protein interaction and repression of reporter gene expression, the IC_{50} of G3335 was 8.67 μM and 31.9 μM, respectively. In contrast, our peptide antagonists possess nanomolar affinity for the PPAR LBDs and a very high degree of specificity for the PPARs over other nuclear receptors, both of which are requisite for their use *in vivo*.

Interestingly, 98% of the PPAR-interacting peptides that we identified also interact directly with activated RXRα bound to 9cisRA. We have previously shown the same to be the case for LRH-1-interacting peptides (29). Although most of our PPAR peptides interact with RXRα in a ligand-dependent manner, the PPAR-selective peptide NBM131 does not inhibit transcription of RXRα or of any of the other receptors that heterodimerize with RXRα. These data suggest that the peptides may interact with another surface on RXRα that is exposed upon ligand binding, or that they lack the high affinity for RXRα needed to compete with coactivators for binding.

We have demonstrated that PPARγ1 prefers peptides that have a very strong consensus binding motif consisting of HPLLXXLL. Although it has been demonstrated previously that residues C-terminal to the LXXLL motif play important roles in binding to PPARγ1 and other nuclear receptors, no consensus emerged in the amino acids C-terminal to the LXXLL within the peptides that we identified (21). The amino acids in the -1 and -2 positions with respect to the LXXLL motif have been shown to stabilize the nuclear receptor-coactivator interaction through various noncovalent interactions, including hydrogen bonding, van der Waals forces, and salt bridge formation (25). From peptide phage display screens performed with other nuclear receptors, it has become clear that residues in the -1 and -2 positions correlate with receptor-binding specificity (23–29, 52). However, no consensus correlating the nature of the -3 amino acid with receptor-binding specificity has been previously established.

Our molecular modeling predicts that the -3 histidine found within our HPLLXXLL motif interacts with two residues within PPARγ1: K319 and E471. E471 forms one end of the charge clamp, and mutation of this residue abrogates interaction of our peptides with PPARγ1. Furthermore, our data predict that the binding of the peptides to PPARγ1 is stabilized by a salt bridge between the -3 histidine of the peptide and K319 of PPARγ1. K319 in helix 4 is important for the

EXHIBIT J

formation of an intramolecular bond with D475 in helix 12 of PPARγ1, and this may contribute to stabilization of helix 12 and coactivator binding (53). Indeed, K319 may form a hydrogen bond with H687 that is found at the −3 position with respect to the second LXXLL motif of SRC-1 (amino acids 690–694), which may explain why the K319A mutant has lower constitutive activity (53, 54). We found that the K319A mutation significantly reduces the interaction between apo- and ligand-activated PPARγ1 and NBM242, suggesting that K319 may be important for stabilizing interactions of the receptor with coactivators in both the absence and presence of ligand. In addition, K319 is a conserved residue in PPARα, PPARγ, and PPARδ, a fact that may explain why the peptides we isolated bind to all three PPAR subtypes.

The high level of constitutive activity is an interesting aspect of PPARγ1 biology. The lack of available antagonists that can inhibit this constitutive activity has hampered our knowledge of the full array of biological effects of this receptor. The development of peptide antagonists that can repress the constitutive activity of PPARγ1 will advance our knowledge of the biological roles played by this receptor. This will ultimately be important in understanding the therapeutic applications and side effects of PPARγ ligands used clinically.

The etiology of the constitutive activity of PPARγ1 is not altogether clear. Because an endogenous ligand for PPARγ1 has yet to be confirmed, one hypothesis is that in cells, PPARγ1 is bound to a low-affinity fatty acid or other ligand, which causes the recruitment of coactivators responsible for the constitutive activity of PPARγ1 (53). Agonist binding increases the stability of the AF-2 structure, further strengthening the recruitment of coactivators to enhance transcription. It stands to reason that a coactivator with high affinity for the unliganded receptor could increase the constitutive activity of the receptor, obviating the need for any ligand; discovery of a PPAR-binding motif may help identify novel coactivators that can function in this regard. Interestingly, mutation −6 of NBM242 has the ability to bind with high ligand independence. This raises the possibility that the constitutive activity of PPARγ1 could be explained by coactivator recruitment to a conformation of PPARγ1 induced either in the absence of ligand or in the presence of an unconfirmed endogenous ligand. It is worth noting that using NBM239, we are able to partially inhibit the constitutive activity of PPARγ1, demonstrating that the constitutive activity can be partially blocked through the use of LXXLL-containing peptide antagonists of PPARγ1.

It has been suggested that helix 12 of constitutively active nuclear receptors contains amino acids that are required for their high basal activity (53). A heterozygous dominant-negative mutation within helix 12 of PPARγ1, P467L, has previously been associated with early-onset type 2 diabetes mellitus and hypertension (55). This mutation perturbs the orientation and dynamic properties of helix 12, likely resulting in abrogated coactivator recruitment and reduced constitutive PPARγ1 transcriptional activity. Of note, P467 is found within a sequence motif consisting of HPLLQEIY, a conserved motif found in helix 12 of all three PPAR subtypes. Although this motif is not identical to the motif we identified, it is quite similar, especially considering the flexibility in the +4 and +5 positions that we observed. The presence of this motif is interesting especially in light of the finding that the extended helix 12 of one PPARγ molecule in an inactive conformation contacts the charge clamp of another apo-PPARγ molecule in a crystallographically related homodimer that is in an active conformation (54). This finding raises the question of whether this motif is important for the interaction. Whether such an intermolecular interaction involving this motif is relevant to the PPAR/RXR heterodimer is not known.

The results of this study support the hypothesis that targeting the nuclear receptor-coactivator interaction surface could be a viable mechanism of inhibiting nuclear receptor function *in vivo*. In addition to elucidating some of the molecular determinants of PPAR-coactivator interactions, this work lends support for the rational design of peptidomimetics that can be used to target this interaction in the broad range of physiological and pathological processes in which nuclear receptors are implicated.

MATERIALS AND METHODS

Biochemicals

Rosiglitazone, carbaprostacyclin, and 22(R)-OH-cholesterol were purchased from Cayman Chemical (Ann Arbor, MI). Clofibrate, GW7647, 9cisRA, 17β-estradiol, dexamethasone, chenodeoxycholic acid, rifampicin, T_3, and all-trans retinoic acid were purchased from Sigma-Aldrich (St. Louis, MO). Methyltrienolone (R1881) and promegestone (R5020) were purchased from PerkinElmer, Inc. (Waltham, MA). 1,25-Dihydroxy-vitamin D_3 was purchased from BIOMOL International, L.P. (Plymouth Meeting, PA). GW7845 was a gift from GlaxoSmithKline (Research Triangle Park, NC). Mutagenesis and quantitative PCR oligonucleotides were obtained from Integrated DNA Technologies (Coralville, IA).

Plasmids

Cytomegalovirus (CMV)-βgal was purchased from CLONTECH Laboratories, Inc. (Mountain View, CA). pBSII was purchased from Stratagene (La Jolla, CA). Mammalian expression constructs for nuclear receptors were obtained as described previously (56). cDNAs for PPARs were obtained: PPARγ1 (B. Spiegelman), PPARδ (GlaxoSmithKline), and PPARα (HepG2 cells). Mammalian expression vectors pcDNA3.1nV5-PPARγ1, VP16-GwA, VP16-GwA-PPARγ1, VP16-GwA-PPARγ2, VP16-GwA-PPARδ, and VP16-GwA-PPARα were constructed as described previously (58). The nuclear receptor reporter genes used were: 3X-ERE-tata-Luc (for ERα, ERβ, ERRα, ERRβ, and ERRγ) (57), DR1-Luc (for PPARγ1, RXRα, and hepatocyte nuclear factor-4α2) (R. Heyman), mouse mammary tumor virus-Luc (for AR and progesterone receptor), SHP-1400-Luc (for LRH-1) (S. Kliewer), DR5-tk-Luc (for RARα) and LXRE-tk-Luc (for liver X receptor α) (D. Mangelsdorf), and 5XGal4TataLuc3 (25). The PEPCK

EXHIBIT J

(−2000/+73)-luciferase reporter gene was a gift from Dr. Edwards A. Park (University of Tennessee Health Science Center, Memphis, TN). pM-PGC1αL2 was constructed as described previously (30). Peptides were cloned into pM5.1, a vector derived from pM (CLONTECH) that enables the peptides to be cloned as N-terminal fusions to the Gal4DBD. The mutations of NBM242 and the K319A and E471A mutations of PPARγ1 were generated by QuikChange Site-Directed Mutagenesis Kit (Stratagene) using primers with the desired mutations. All PCR products were sequenced to ensure the fidelity of the resulting constructs.

Production and Purification of Full-Length Recombinant hPPARγ1 and hRXRα and DNA-Binding Assay

hPPARγ1 and hRXRα were purified as previously described for the purification of other nuclear receptors (37). After expression of the biotinylated proteins in Sf9 insect cells, hPPARγ1 and hRXRα were purified by batch method using monomeric avidin resin (Promega Corp., Madison, WI) or using fast performance liquid chromatography and Streptavidin Mutein Matrix resin (Roche, Indianapolis, IN), as has been previously described. The proteins were run on reducing SDS-PAGE gels and detected by Coomassie blue staining (37). To test the functionality of the purified proteins, a DNA-binding assay was performed. A 96-well plate was prepared as follows: well coated with 10 μg neutravidin (Thermo Fisher Scientific, Inc., Pierce Biotechnology, Rockford, IL) in 100 mM $NaHCO_3$ (pH 8.5) for 2 h at room temperature, blocked for 1 h with 2% milk in $NaHCO_3$, washed five times with PBST (PBS + 0.1% Tween 20), incubated with 2 pmol of double-stranded 5′-biotinylated oligonucleotides (diluted in PBST) containing the aP2 PPRE for 1 h (5Bio-GATCTAAACTAGGTCAAAGGTCATGCG annealed with 5Bio-GATCCGCATGACCTTTGACCTAGTTTA), blocked with 5 mM biotin for 1 h, and washed five times with PBST. Equal molar quantities of purified biotinylated hPPARγ1 and/or purified biotinylated hRXRα (1 μg each) were allowed to bind to the PPRE overnight at 4 C in PBST in the presence of ligand. Ligands used were 1 μM of the nonthiazolidinedione tyrosine-based PPARγ ligand GW7845 or 1 μM 9cisRA. The wells were washed five times with PBST to remove unbound proteins. Proteins were eluted by boiling in Laemmli 4X buffer (Bio-Rad Laboratories, Inc., Hercules, CA), run on a reducing SDS-PAGE gel, and detected by Coomassie blue staining.

Affinity Selection of PPAR Binding Sequences

M13 phage particles displaying PPAR-selective peptides were obtained as described previously (25, 30, 52). In brief, 2 μg of purified baculovirus-expressed, biotinylated, purified hPPARγ1 was diluted in 100 μl of 100 mM $NaHCO_3$ (pH 8.5) and either 1 μM rosiglitazone solubilized in 100% ethanol or the equivalent volume of ethanol. The protein was allowed to bind the plastic wells overnight at 4 C. Alternatively, to prepare wells for screening the DNA-bound hPPARγ1/hRXRα heterodimer, wells of a 96-well plate were prepared as described above for the DNA-binding assay. The wells were treated with approximately 10^{10} phage particles of a phage peptide library preblocked in 100 μl of MPBS (2% nonfat dry milk in PBS) for 1 h, and panning was done as described previously (30). Phage eluted from the target were amplified in *Escherichia coli* DH5αF′ cells (Invitrogen, Carlsbad, CA) for 5 h at 37 C, and the supernatant containing amplified phage was collected for use in subsequent rounds of panning for a total of three rounds of panning. Enrichment of PPAR-binding phage was confirmed by a phage ELISA as described previously (25). PCR amplification of the peptides was performed using 0.4 μl of the amplified phage from bacterial supernatants that showed significant enrichment of target-binding phage. The PCR products were purified and digested with *Xba*I and *Xho*I before ligation into pM5.1 for mammalian two-hybrid analysis. The peptide sequences were deduced by DNA sequencing. Construction of the LXXLL M13 phage library was described previously (25), and the SS-X_{16}-S M13 phage library was a gift from D. J. Kenan (Duke University Medical Center, Durham, NC).

Coactivator-Phage Competition ELISA

A T7 phage expressing the nuclear receptor-interacting fragment of ASC-2 (amino acids 254–321) was obtained from a screen of a T7 library performed in our laboratory (Dwyer, M. A., and D. P. McDonnell, unpublished data). The competition ELISA was performed by immobilizing hPPARγ1 directly on the plastic well overnight at 4 C as described above for the affinity selection of PPAR binding sequences. This was followed by blocking and incubating with a combination of 10^8 pfu of ASC-2 coactivator-phage plus the synthetic NBM239 peptide (see below for details on synthesis) for 3 h. The wells were washed 10 times with PBST, and the bound phage were detected by ELISA, using anti-T7 phage HRP-conjugated antibody (Novagen, San Diego, CA). Bound antibody-enzyme conjugate was detected by 2,2′-azino-bis(3-ethylbenzothiazoline-6-sulfonic acid) (Sigma-Aldrich) in the presence of 0.05% H_2O_2 for 15 min, and absorbance was measured at 405 nm in a Multiskan MS microplate reader (Labsystems, Inc., Helsinki, Finland).

Mammalian Cell Culture and Transient Transfection Assays

HepG2 human hepatoma cells and HeLa human cervical carcinoma cells were obtained from American Type Culture Collection (Manassas, VA), maintained in MEM (Invitrogen) supplemented with 8% fetal bovine serum (HyClone Laboratories, Logan, UT), 0.1 mM nonessential amino acids, and 1 mM sodium pyruvate (Invitrogen) in a humidified 37 C incubator with 5% CO_2. All mammalian two-hybrid analyses were performed in HepG2 cells. Cis-trans assays were performed in HeLa cells. HepG2 cells were seeded in wells of 96- or 24-well plates coated with 0.1% gelatin for 10 min at 25 C. For transient transfections, cells were split in 24- or 96-well plates 24 h before transfection. On the day of transfection, the medium was aspirated and cells were washed once with PBS. Cells were transfected with 3 μg of total plasmid per triplicate sample in 24-well or 600 ng in 96-well plate format, using Lipofectin according to manufacturer's protocol (Invitrogen). DNA-Lipofectin mix was added and incubated for 5 h (HepG2) or 4 h (HeLa). The transfection was stopped by aspirating the DNA-Lipofectin mix and replacing with phenol red-free MEM (Invitrogen) supplemented with 8% charcoal-stripped serum (HyClone), nonessential amino acids, and sodium pyruvate (Invitrogen). All ligand stocks were dissolved in ethanol or DMSO before use in cell culture, and cells were treated with ligands added to phenol red-free MEM. A saturating concentration of ligand was added to the cells either immediately or 24 h post-transfection: 1 μM rosiglitazone (for PPARγ), 10 μM carbaprostacyclin (for PPARδ), 100 μM clofibrate (for PPARα), 100 nM GW7647 (for PPARα), 1 μM 9cisRA (for RXRα), 100 nM 17β-estradiol (for ERα and ERβ), 100 nM all-trans retinoic acid (for RARα), 10 nM R1881 (for AR), 100 nM dexamethasone (for glucocorticoid receptor), 100 nM R5020, 100 nM T3, 100 nM 1,25-dihydroxy-vitamin D_3, 50 μM chenodeoxycholic acid (for farnesoid X receptor), 10 μM 22(R)-OH-cholesterol (for LXR), and 10 μM rifampicin (for PXR). Cells were lysed 40–48 h after transfection and assayed for luciferase and β-galactosidase activities using a Fusion Universal Microplate Analyzer (PerkinElmer). Results are expressed as normalized luciferase activity (NLA, normalized with βgal for transfection efficiency) ± SEM per triplicate sample of cells. Results presented were typical of three independent transfection experiments, each performed with triplicates of each experimental condition.

EXHIBIT J

Molecular Modeling Studies

Structural models of PPARγ LBD in complex with the NBM242 peptide were generated using Pymol molecular graphics and modeling package (41) and the crystal structure coordinates of the LBD of PPARγ in complex with the SRC-1 peptide (PDB: 1FM6) (42). The residues of the SRC-1 peptide were mutated *in silico* to the residues of the NBM242 peptide, and the most frequently occurring amino acid rotamer was selected.

Western Blot Analysis

HepG2 cells were transfected or infected as indicated, and after 48 h, cells were lysed in X-400 buffer containing 20 mM HEPES (pH 7.9), 20% glycerol, 400 mM KCl, 1 mM EDTA, 1 mM dithiothreitol, and Protease Inhibitor Cocktail 3 (Calbiochem, San Diego, CA). Laemmli 4X buffer (Bio-Rad) was added to the samples after Bradford protein estimation (Bio-Rad). The samples were boiled for 10 min at 95 C, loaded on a reducing SDS-PAGE gel, and transferred to nitrocellulose membrane (Amersham, Buckinghamshire, UK). Expression of peptides was detected with the anti-Gal4DBD antibody sc577 diluted 1:500 in MPBST (Santa Cruz Biotechnology, Inc., Santa Cruz, CA) and antirabbit IgG HRP-conjugated secondary antibody NA934 diluted 1:4000 in MPBST (Amersham). Expression of PPARγ1, PPARγ1K319A, and PPARγ1E471A was detected with the anti-PPARγ antibody E-8 diluted 1:1000 in MPBST (Santa Cruz Biotechnology, Inc.) and antimouse IgG HRP-conjugated antibody NA931 diluted 1:4000 in MPBST (Amersham).

Preparation of Synthetic Peptides

Peptides were synthesized by standard Fmoc protocol on PAL-PEG-PS resin (Applied Biosystems, Foster City, CA) utilizing a 396 MPS automated peptide synthesizer (Advanced ChemTech, Louisville, KY). All peptides were cleaved from the resin with 95% trifluoroacetic acid, 2.5% water, and 2.5% triisopropylsilane, yielding an amide on the peptide's C terminus. Purification was done by reverse-phase HPLC with a Vydac C18 column and a gradient elution by solvents A (99% H_2O, 1% CH_3CN, and 0.1% trifluoroacetic acid) and B (95% CH_3CN, 5% H_2O, and 0.1% trifluoroacetic acid). Molecular mass and purity were confirmed via LCMS-ESI. Peptides were then lyophilized and stored at −80 C.

Fluorescence Polarization

5-FAM-labeled fluorescent peptides were ordered with a cysteine at the C terminus (American Peptide Co., Inc., Sunnyvale, CA). Mass spectral analysis by electrospray and HPLC analysis revealed peptides of correct molecular weight with purities between 95.3% and 97.5%. The peptides were solubilized in water to a concentration of 1 mg/ml. The buffer used to dilute the protein and peptides contained 10 mM HEPES (pH 7.4), 150 mM NaCl, 3 mM EDTA, 0.005% Tween 20. Fluorescence polarization was measured using the PerkinElmer α-HT FP machine (PerkinElmer) with excitation at 485 nm and emission at 535 nm for fluoresceinated peptides. Data presented are the average of two independent experiments.

Adenoviral Construction and Infection

Adenoviruses expressing NBM131 or NBM131mut4 were generated using the ViraPower Adenoviral Expression System according to manufacturer's protocol (Invitrogen). In brief, viruses were made by subcloning the peptide-Gal4DBD fusions into pENTR-D-TOPO (Invitrogen), followed by recombination into pAd/CMV/V5-DEST (Invitrogen). The *Pac*I-digested pAd/CMV/V5-DEST constructs containing either NBM131 or NBM131mut4 were transfected using FuGENE 6 (Roche) in 293A cells (Invitrogen), and adenoviruses were produced. Recombinant adenoviruses were purified by CsCl density gradient centrifugation. The purified virus stocks were desalted over Sephadex G-25 columns (Amersham) and eluted in sterile PBS. Glycerol was added for a final concentration of 10%, and the virus stocks were aliquoted and stored at −80 C until used. Infectious viral titers were calculated using the end-point dilution assay. HepG2 cells were infected with adenoviruses by diluting the purified adenovirus to MOI 20 in a small volume of media and infecting cells on a rocker at room temperature for 2 h. The infection was stopped by aspirating the virus-containing media and replacing with fresh growth media. Twenty-four hours after infection, cells were treated with ligand for 24 h, and RNA was harvested for quantitative PCR analysis.

RNA Isolation and Quantitative Real-time PCR

For RNA isolation, HepG2 cells were seeded in six-well plates in MEM as described above. Cells were infected 24 h after plating. Twenty-four hours after infection, cells were treated with 1 μM rosiglitazone or 100 nM GW7647 for an additional 24 h. Cells were then harvested and total RNA of HepG2 cells was isolated using Aurum Total RNA Kit according to manufacturer's protocol (Bio-Rad). Total RNA (1 μg) was reverse transcribed using the iScript cDNA synthesis kit (Bio-Rad). Quantitative PCR was performed using the Bio-Rad iCycler Realtime PCR System (Bio-Rad) using 0.1 μl cDNA, 10 μM each primer, and iQ SYBR Green Supermix detection reagent (Bio-Rad). Data are the mean ± SEM of triplicate samples. A control sample without reverse transcriptase was performed to exclude genomic DNA contamination. The melt curves for each primer were also obtained to confirm that a single amplicon was obtained. The expression data were normalized to the endogenous control acidic ribosomal phosphoprotein P0 (36B4). The expression of 36B4 was not affected by adenoviral infection or by treatments. The primers were designed using GenScript or IDT Primer Quest Tool. The sequences of the primers are listed in supplemental Fig. 1F.

Acknowledgments

We thank members of the McDonnell laboratory for critical reading of this manuscript. The SS-X_{16}-S M13 phage library was a generous gift from Dr. Daniel J. Kenan (Duke University Medical Center, Durham, NC). The nuclear receptor LBDs, fluorescent peptides, and PPARγ agonist GW7845 were generous gifts from GlaxoSmithKline (Research Triangle Park, NC). PEPCK (−2000/+73)-luciferase reporter gene was a generous gift from Dr. Edwards A. Park (University of Tennessee Health Science Center, Memphis, TN).

Received April 20, 2007. Accepted June 20, 2007.

Address all correspondence and requests for reprints to: Donald P. McDonnell, Duke University Medical Center, Pharmacology and Cancer Biology, Box 3813, Durham, North Carolina 27710. E-mail: donald.mcdonnell@duke.edu.

This work was supported by Department of Defense Breast Cancer Research Program Award W81XWH-05-1-0251 (to N.B.M.), and National Institutes of Health Grant DK48807 (to D.P.M.).

Disclosure Statement: N.B.M., T.B.S., M.A.D., M.S.J., J.E.A., and J.M.H. have nothing to declare. D.P.M. consults for and has received lecture fees from Wyeth Pharmaceuticals. D.P.M. consults for Ligand Pharmaceuticals. D.P.M. has received research support from GlaxoSmithKline.

EXHIBIT J

REFERENCES

1. Gottlicher M, Widmark E, Li Q, Gustafsson JA 1992 Fatty acids activate a chimera of the clofibric acid-activated receptor and the glucocorticoid receptor. Proc Natl Acad Sci USA 89:4653–4657
2. Dreyer C, Keller H, Mahfoudi A, Laudet V, Krey G, Wahli W 1993 Positive regulation of the peroxisomal β-oxidation pathway by fatty acids through activation of peroxisome proliferator-activated receptors (PPAR). Biol Cell 77:67–76
3. Mandard S, Muller M, Kersten S 2004 Peroxisome proliferator-activated receptor α target genes. Cell Mol Life Sci 61:393–416
4. Issemann I, Green S 1990 Activation of a member of the steroid hormone receptor superfamily by peroxisome proliferators. Nature 347:645–650
5. Burdick AD, Kim DJ, Peraza MA, Gonzalez FJ, Peters JM 2006 The role of peroxisome proliferator-activated receptor-β/δ in epithelial cell growth and differentiation. Cell Signal 18:9–20
6. Barak Y, Liao D, He W, Ong ES, Nelson MC, Olefsky JM, Boland R, Evans RM 2002 Effects of peroxisome proliferator-activated receptor δ on placentation, adiposity, and colorectal cancer. Proc Natl Acad Sci USA 99: 303–308
7. Barish GD, Narkar VA, Evans RM 2006 PPAR δ: a dagger in the heart of the metabolic syndrome. J Clin Invest 116:590–597
8. Burdick AD, Bility MT, Girroir EE, Billin AN, Willson TM, Gonzalez FJ, Peters JM 2007 Ligand activation of peroxisome proliferator-activated receptor-β/δ(PPARβ/δ) inhibits cell growth of human N/TERT-1 keratinocytes. Cell Signal 19:1163–1171
9. Tontonoz P, Hu E, Graves RA, Budavari AI, Spiegelman BM 1994 mPPAR γ 2: tissue-specific regulator of an adipocyte enhancer. Genes Dev 8:1224–1234
10. Tontonoz P, Hu E, Spiegelman BM 1994 Stimulation of adipogenesis in fibroblasts by PPAR γ 2, a lipid-activated transcription factor. Cell 79:1147–1156
11. Chawla A, Schwarz EJ, Dimaculangan DD, Lazar MA 1994 Peroxisome proliferator-activated receptor (PPAR) γ: adipose-predominant expression and induction early in adipocyte differentiation. Endocrinology 135:798–800
12. Forman BM, Tontonoz P, Chen J, Brun RP, Spiegelman BM, Evans RM 1995 15-Deoxy-δ 12, 14-prostaglandin J2 is a ligand for the adipocyte determination factor PPAR γ. Cell 83:803–812
13. Kliewer SA, Lenhard JM, Willson TM, Patel I, Morris DC, Lehmann JM 1995 A prostaglandin J2 metabolite binds peroxisome proliferator-activated receptor γ and promotes adipocyte differentiation. Cell 83:813–819
14. Kliewer SA, Sundseth SS, Jones SA, Brown PJ, Wisely GB, Koble CS, Devchand P, Wahli W, Willson TM, Lenhard JM, Lehmann JM 1997 Fatty acids and eicosanoids regulate gene expression through direct interactions with peroxisome proliferator-activated receptors α and γ. Proc Natl Acad Sci USA 94:4318–4323
15. Krey G, Braissant O, L'Horset F, Kalkhoven E, Perroud M, Parker MG, Wahli W 1997 Fatty acids, eicosanoids, and hypolipidemic agents identified as ligands of peroxisome proliferator-activated receptors by coactivator-dependent receptor ligand assay. Mol Endocrinol 11: 779–791
16. Brown PJ, Stuart LW, Hurley KP, Lewis MC, Winegar DA, Wilson JG, Wilkison WO, Ittoop OR, Willson TM 2001 Identification of a subtype selective human PPARα agonist through parallel-array synthesis. Bioorg Med Chem Lett 11:1225–1227
17. Gupta RA, Tan J, Krause WF, Geraci MW, Willson TM, Dey SK, DuBois RN 2000 Prostacyclin-mediated activation of peroxisome proliferator-activated receptor δ in colorectal cancer. Proc Natl Acad Sci USA 97: 13275–13280
18. Lin BC, Hong SH, Krig S, Yoh SM, Privalsky ML 1997 A conformational switch in nuclear hormone receptors is involved in coupling hormone binding to corepressor release. Mol Cell Biol 17:6131–6138
19. Privalsky ML 2004 The role of corepressors in transcriptional regulation by nuclear hormone receptors. Annu Rev Physiol 66:315–360
20. Heery DM, Kalkhoven E, Hoare S, Parker MG 1997 A signature motif in transcriptional co-activators mediates binding to nuclear receptors. Nature 387:733–736
21. McInerney EM, Rose DW, Flynn SE, Westin S, Mullen TM, Krones A, Inostroza J, Torchia J, Nolte RT, Assa-Munt N, Milburn MV, Glass CK, Rosenfeld MG 1998 Determinants of coactivator LXXLL motif specificity in nuclear receptor transcriptional activation. Genes Dev 12:3357–3368
22. Wu Y, Chin WW, Wang Y, Burris TP 2003 Ligand and coactivator identity determines the requirement of the charge clamp for coactivation of the peroxisome proliferator-activated receptor γ. J Biol Chem 278:8637–8644
23. Norris JD, Paige LA, Christensen DJ, Chang CY, Huacani MR, Fan D, Hamilton PT, Fowlkes DM, McDonnell DP 1999 Peptide antagonists of the human estrogen receptor. Science 285:744–746
24. McDonnell DP, Chang CY, Norris JD 2000 Development of peptide antagonists that target estrogen receptor-cofactor interactions. J Steroid Biochem Mol Biol 74: 327–335
25. Chang C, Norris JD, Gron H, Paige LA, Hamilton PT, Kenan DJ, Fowlkes D, McDonnell DP 1999 Dissection of the LXXLL nuclear receptor-coactivator interaction motif using combinatorial peptide libraries: discovery of peptide antagonists of estrogen receptors α and β. Mol Cell Biol 19:8226–8239
26. Hall JM, Chang CY, McDonnell DP 2000 Development of peptide antagonists that target estrogen receptor β-coactivator interactions. Mol Endocrinol 14:2010–2023
27. Chang CY, Abdo J, Hartney T, McDonnell DP 2005 Development of peptide antagonists for the androgen receptor using combinatorial peptide phage display. Mol Endocrinol 19:2478–2490
28. Zella LA, Chang CY, McDonnell DP, Wesley Pike J 2007 The vitamin D receptor interacts preferentially with DRIP(205)-like LxxLL motifs. Arch Biochem Biophys 460: 206–212
29. Safi R, Kovacic A, Gaillard S, Murata Y, Simpson ER, McDonnell DP, Clyne CD 2005 Coactivation of liver receptor homologue-1 by peroxisome proliferator-activated receptor γ coactivator-1α on aromatase promoter II and its inhibition by activated retinoid X receptor suggest a novel target for breast-specific antiestrogen therapy. Cancer Res 65:11762–11770
30. Gaillard S, Dwyer MA, McDonnell DP 2007 Definition of the molecular basis for estrogen receptor-related receptor-α-cofactor interactions. Mol Endocrinol 21:62–76
31. Huang HJ, Norris JD, McDonnell DP 2002 Identification of a negative regulatory surface within estrogen receptor α provides evidence in support of a role for corepressors in regulating cellular responses to agonists and antagonists. Mol Endocrinol 16:1778–1792
32. Zhu Y, Qi C, Calandra C, Rao MS, Reddy JK 1996 Cloning and identification of mouse steroid receptor coactivator-1 (mSRC-1), as a coactivator of peroxisome proliferator-activated receptor γ. Gene Expr 6:185–195
33. Puigserver P, Wu Z, Park CW, Graves R, Wright M, Spiegelman BM 1998 A cold-inducible coactivator of nuclear receptors linked to adaptive thermogenesis. Cell 92:829–839
34. Yuan CX, Ito M, Fondell JD, Fu ZY, Roeder RG 1998 The TRAP220 component of a thyroid hormone receptor-associated protein (TRAP) coactivator complex interacts

EXHIBIT J

directly with nuclear receptors in a ligand-dependent fashion. Proc Natl Acad Sci USA 95:7939–7944
35. Issemann I, Prince RA, Tugwood JD, Green S 1993 The retinoid X receptor enhances the function of the peroxisome proliferator activated receptor. Biochimie 75: 251–256
36. Keller H, Dreyer C, Medin J, Mahfoudi A, Ozato K, Wahli W 1993 Fatty acids and retinoids control lipid metabolism through activation of peroxisome proliferator-activated receptor-retinoid X receptor heterodimers. Proc Natl Acad Sci USA 90:2160–2164
37. Juzumiene D, Chang CY, Fan D, Hartney T, Norris JD, McDonnell DP 2005 Single-step purification of full-length human androgen receptor. Nucl Recept Signal 3:e001
38. Suh N, Wang Y, Williams CR, Risingsong R, Gilmer T, Willson TM, Sporn MB 1999 A new ligand for the peroxisome proliferator-activated receptor-γ (PPAR-γ), GW7845, inhibits rat mammary carcinogenesis. Cancer Res 59:5671–5673
39. Levin AA, Sturzenbecker LJ, Kazmer S, Bosakowski T, Huselton C, Allenby G, Speck J, Kratzeisen C, Rosenberger M, Lovey A, Grippo JF 1992 9-cis retinoic acid stereoisomer binds and activates the nuclear receptor RXR α. Nature 355:359–361
40. Kliewer SA, Umesono K, Noonan DJ, Heyman RA, Evans RM 1992 Convergence of 9-cis retinoic acid and peroxisome proliferator signalling pathways through heterodimer formation of their receptors. Nature 358: 771–774
41. DeLano WL 2002 The PyMOL Molecular Graphics System. Palo Alto, CA: DeLano Scientific
42. Gampe Jr RT, Montana VG, Lambert MH, Miller AB, Bledsoe RK, Milburn MV, Kliewer SA, Willson TM, Xu HE 2000 Asymmetry in the PPARγ/RXRα crystal structure reveals the molecular basis of heterodimerization among nuclear receptors. Mol Cell 5:545–555
43. Gerhold DL, Liu F, Jiang G, Li Z, Xu J, Lu M, Sachs JR, Bagchi A, Fridman A, Holder DJ, Doebber TW, Berger J, Elbrecht A, Moller DE, Zhang BB 2002 Gene expression profile of adipocyte differentiation and its regulation by peroxisome proliferator-activated receptor-γ agonists. Endocrinology 143:2106–2118
44. Rodriguez JC, Gil-Gomez G, Hegardt FG, Haro D 1994 Peroxisome proliferator-activated receptor mediates induction of the mitochondrial 3-hydroxy-3-methylglutaryl-CoA synthase gene by fatty acids. J Biol Chem 269: 18767–18772
45. Arnold LA, Estebanez-Perpina E, Togashi M, Jouravel N, Shelat A, McReynolds AC, Mar E, Nguyen P, Baxter JD, Fletterick RJ, Webb P, Guy RK 2005 Discovery of small molecule inhibitors of the interaction of the thyroid hormone receptor with transcriptional coregulators. J Biol Chem 280:43048–43055
46. Huang H, Wang H, Sinz M, Zoeckler M, Staudinger J, Redinbo MR, Teotico DG, Locker J, Kalpana GV, Mani S 2007 Inhibition of drug metabolism by blocking the activation of nuclear receptors by ketoconazole. Oncogene 26:258–268
47. Denicourt C, Dowdy SF 2004 Medicine. Targeting apoptotic pathways in cancer cells. Science 305:1411–1413
48. Kieber-Emmons T, Murali R, Greene MI 1997 Therapeutic peptides and peptidomimetics. Curr Opin Biotechnol 8:435–441
49. Melikov K, Chernomordik LV 2005 Arginine-rich cell penetrating peptides: from endosomal uptake to nuclear delivery. Cell Mol Life Sci 62:2739–2749
50. Fernandez-Carneado J, Kogan MJ, Pujals S, Giralt E 2004 Amphipathic peptides and drug delivery. Biopolymers 76:196–203
51. Ye F, Zhang ZS, Luo HB, Shen JH, Chen KX, Shen X, Jiang HL 2006 The dipeptide H-Trp-Glu-OH shows highly antagonistic activity against PPARγ: bioassay with molecular modeling simulation. Chembiochem 7:74–82
52. Chang CY, Norris JD, Jansen M, Huang HJ, McDonnell DP 2003 Application of random peptide phage display to the study of nuclear hormone receptors. Methods Enzymol 364:118–142
53. Molnar F, Matilainen M, Carlberg C 2005 Structural determinants of the agonist-independent association of human peroxisome proliferator-activated receptors with coactivators. J Biol Chem 280:26543–26556
54. Nolte RT, Wisely GB, Westin S, Cobb JE, Lambert MH, Kurokawa R, Rosenfeld MG, Willson TM, Glass CK, Milburn MV 1998 Ligand binding and co-activator assembly of the peroxisome proliferator-activated receptor-γ. Nature 395:137–143
55. Barroso I, Gurnell M, Crowley VE, Agostini M, Schwabe JW, Soos MA, Maslen GL, Williams TD, Lewis H, Schafer AJ, Chatterjee VK, O'Rahilly S 1999 Dominant negative mutations in human PPARγ associated with severe insulin resistance, diabetes mellitus and hypertension. Nature 402:880–883
56. Gaillard S, Grasfeder LL, Haeffele CL, Lobenhofer EK, Chu TM, Wolfinger R, Kazmin D, Koves TR, Muoio DM, Chang CY, McDonnell DP 2006 Receptor-selective coactivators as tools to define the biology of specific receptor-coactivator pairs. Mol Cell 24:797–803
57. Tzukerman MT, Esty A, Santiso-Mere D, Danielian P, Parker MG, Stein RB, Pike JW, McDonnell DP 1994 Human estrogen receptor transactivational capacity is determined by both cellular and promoter context and mediated by two functionally distinct intramolecular regions. Mol Endocrinol 8:21–30
58. Hall JM, McDonnell DP 2007 The molecular mechanisms underlying the proinflammatory actions of thiazolidinediones in human macrophages. Mol Endocrinol 21:1756–1768

Molecular Endocrinology **is published monthly by The Endocrine Society (http://www.endo-society.org), the foremost professional society serving the endocrine community.**